Research Article

Altered electroencephalographic networks in developmental dyslexia after remedial training: a prospective case-control study

https://doi.org/10.4103/1673-5374.295334

Received: February 21, 2020

Peer review started: March 2, 2020

Accepted: July 22, 2020

Published online: October 9, 2020

Juliana A. Dushanova*, Stefan A. Tsokov

Graphical Abstract *The neural networks in children with developmental dyslexia reorganize after a remedial training with visual tasks*

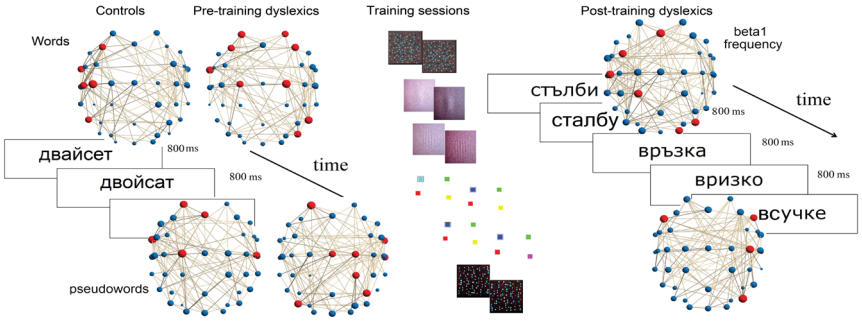

Abstract

Electroencephalographic studies using graph theoretic analysis have found aberrations in functional connectivity in children with developmental dyslexia. However, how the training with visual tasks can change the functional connectivity of the semantic network in developmental dyslexia is still unclear. We looked for differences in local and global topological properties of functional networks between 21 healthy controls and 22 dyslexic children (8–9 years old) before and after training with visual tasks in this prospective case-control study. The minimum spanning tree method was used to construct the subjects' brain networks in multiple electroencephalographic frequency ranges during a visual word/pseudoword discrimination task. We found group differences in the theta, alpha, beta and gamma bands for four graph measures suggesting a more integrated network topology in dyslexics before the training compared to controls. After training, the network topology of dyslexic children had become more segregated and similar to that of the controls. In the θ, α and β1-frequency bands, compared to the controls, the pre-training dyslexics exhibited a reduced degree and betweenness centrality of the left anterior temporal and parietal regions. The simultaneous appearance in the left hemisphere of hubs in temporal and parietal (α, β1), temporal and superior frontal cortex (θ, α), parietal and occipitotemporal cortices (β1), identified in the networks of normally developing children was not present in the brain networks of dyslexics. After training, the hub distribution for dyslexics in the theta and beta1 bands had become similar to that of the controls. In summary, our findings point to a less efficient network configuration in dyslexics compared to a more optimal global organization in the controls. This is the first study to investigate the topological organization of functional brain networks of Bulgarian dyslexic children. Approval for the study was obtained from the Ethics Committee of the Institute of Neurobiology and the Institute for Population and Human Studies, Bulgarian Academy of Sciences (approval No. 02-41/12.07.2019) on March 28, 2017, and the State Logopedic Center and the Ministry of Education and Science (approval No. 09-69/14.03.2017) on July 12, 2019.

Key Words: adjusted post-training network; developmental dyslexia; EEG; frequency oscillations; functional connectivity; visual training tasks; visual word/pseudoword discrimination

Chinese Library Classification No. R493; R741

Introduction

The human brain can be regarded as a complex network of neurons or neuronal populations and the connections between them. On a large scale, this can lead to the emergence of highly complex connectivity patterns between functionally diverse components. These "functional" connectivities can be studied through the statistical dependencies between the different functional components (Bassett and Bullmore, 2006). Often brain networks are studied in terms of functional segregation and integration. Functional segregation reflects the ability of the brain to process specific information locally, i.e. within a brain region or an interconnected group of adjacent regions, whereas functional integration is the ability to combine information from different brain regions (Tewarie et al., 2015). Graph theory is a useful mathematical tool in the study of brain

Institute of Neurobiology, Bulgarian Academy of Sciences, Sofia, Bulgaria
*Correspondence to: Juliana A. Dushanova, PhD, juliana@bio.bas.bg.
https://orcid.org/0000-0002-0253-6568 (Juliana A. Dushanova)

Funding: *The study was supported by a grant from the National Science Fund of the Ministry of Education and Science (project DN05/14-2016, to JAD).*
How to cite this article: *Dushanova JA, Tsokov SA (2021) Altered electroencephalographic networks in developmental dyslexia after remedial training: a prospective case-control study. Neural Regen Res 16(4):734-743.*

networks. It describes networks as a set of nodes and their connections (links, edges). Brain network integration and segregation can be characterized by graph measures. Brain networks have been shown to exhibit small-world properties (Bassett and Bullmore, 2006). Small-world networks combine high local connectedness with high global integration (Watts and Strogatz, 1998). The small-world model has been used in the study of the topological reorganization of functional brain networks during normal brain development (He et al., 2019). During normal development, the brain networks shift from having a random topology to having a more segregated small-world topology. Recent studies have shown that brain networks contain areas of densely interconnected hubs, called rich clubs (Sporns, 2013). The brain networks process the information in segregated modules, while the most important nodes, the hubs, play a role in the integration of the information across the network.

The study of the topology of functional brain networks can play an important part in understanding the human brain, its normal functioning, its pathology, and its development. One of the important childhood disorders is developmental dyslexia (DD), which is characterized by difficulties in the development of reading, writing, and spelling skills, despite normal intellectual abilities (World Federation of Neurology, 1968). Resting-state brain networks of DD have been well studied using an electroencephalogram (EEG; Fraga González et al., 2016; He et al., 2019). EEG studies of the functional neural networks of developmental dyslexics during the performance of tasks are lacking.

Although developmental dyslexia has been studied extensively on a behavioral level, there is no consensus regarding its causes. Different behavioral studies have found various deficits in the sensitivity to a coherence motion perception, velocity discrimination, motion direction encoding, contrast sensitivity to stimuli with low-/high-spatial frequency in external noise, that selectively associated with low accuracy or with slow performance on reading sub-skills, problems with clearly seeing letters and their order, orienting and focusing of visual-spatial attention (Wilmer et al., 2004; Benassi et al., 2010; Boets et al., 2011; Stein, 2014; Lalova et al., 2018). The efficacy of intervention efforts has also been studied (Lawton, 2011, 2016; Chouake et al., 2012; Qian and Bi, 2015; Lawton and Shelley-Tremblay, 2017; Lalova et al., 2019). More studies are needed to establish the neurophysiological causes of dyslexia. Some studies have focused on investigating the changes in the activity of specific brain regions (Shaywitz et al., 1998; Habib, 2000; Goswami, 2015), however recent research suggests that the causes of the deficits may lie in impaired connectivity between specific brain regions (Fraga González et al., 2016). Various fMRI studies have shown that dyslexics exhibit impaired functional brain networks and that the impairment correlates with the cognitive deficits and their severity (Wolf et al., 2010; Horowitz-Kraus and Holland, 2015; Schurz et al., 2015).

It has been established that human semantic knowledge is supported by a large brain subnetwork, encompassing many different brain regions and coordinated by a central hub or hubs. Among the candidates for these semantic hubs are the anterior temporal lobe, the posterior inferior parietal lobe (particularly the angular gyrus), the middle temporal gyrus and the inferior frontal gyrus (IFG) (Binder et al., 2009; Farahibozorg et al., 2019). The dynamics of the heteromodal semantic network and the roles of the hubs have been investigated by neuro-computational modeling (Tomasello et al., 2017) as well as experimentally using visually presented words (Farahibozorg et al., 2019). The question is whether (or not) methods based on graph theory can be used as a screening test for developmental dyslexia and can they also shed light on the neurophysiological causes behind the observed effectiveness of remedial training with visual tasks (Wilmer et al., 2004; Lawton, 2011; Ebrahimi et al., 2019; Lalova et al., 2019). The hypothesis of this study is that remedial visual task training of dyslexic children can lead to changes in their brain networks, making them more similar to the ones of the controls.

We also hypothesize that these changes would be mainly related to the dorsal pathway, which in turn may influence the functioning of the semantic network. The aim of the present work was to determine, whether: (1) the functional neural network shows a difference in hub distribution between controls and children with DD during a visual semantic task, (2) the neural networks in children with DD may reorganize after remedial training.

Participants and Methods

Study design

A longitudinal study was conducted in the schools that involved repeated observations of the same dyslexic children over a long period. In this observational study with the exposure of visual intervention in non-trial research, the dyslexics are then followed out over time to observe the outcome from the visual training and evaluate the extent to which the visual tasks contribute to the alteration of this childhood disorder (see **Additional file 1** for a design protocol in the subject information sheet).

Participants

Reliable electrophysiological data were obtained from 43 children (**Figure 1**): 22 children with dyslexia (12 boys and 10 girls) and 21 normal children (11 boys and 10 girls). The age range for both groups was 8–9 years from a second grade of four primary schools located in the urban community of middle-level socio-economic status in Sofia, Bulgaria (**Additional Table 1**). Data, collected from July to December 2019, were taken into consideration. All children's parents gave informed consent (**Additional file 1**) for an EEG in accordance with the *Declaration of Helsinki*. The study was approved by the Ethics Committee of the Institute of Neurobiology and the Institute for Population and Human Studies, Bulgarian Academy of Sciences (approval No. 02-41/12.07.2019), and the State Logopedic Center and the Ministry of Education and Science (approval No. 09-69/14.03.2017) (**Additional file 2**) and followed the STrengthening the Reporting of OBservational studies in Epidemiology (STROBE) statement (**Additional file 3**). All participants in the study spoke Bulgarian as their first language. All children were right-handed. The handedness was assessed by a classification of hand preference (Annett, 1970). All participants had non-verbal intelligence scores of 98 or higher (Raven et al., 1998; **Additional Table 1**). All children had a normal or corrected-to-normal vision after an examination by an ophthalmologist. The controls were paid for participating.

The children underwent a series of tests, including neuropsychological tests (Raichev et al., 2005), a DDE-2 battery for evaluation of developmental dyslexia and dysorthography (Sartori et al., 2007; Matanova and Todorova, 2013), psychometric tests for the evaluation of phonological awareness, tests for the evaluation of reading and writing skills (Kalonkina and Lalova, 2016), Girolami-Boulinier's "Different Oriented Marks" nonverbal perception test (Girolami-Boulinier, 1985; Yakimova, 2004), and Raven's Progressive Matrices test for nonverbal intelligence (Raven et al., 1998). In the dyslexic group were included children with reading difficulties combined with below-norm performance in either speed or accuracy below one standard deviation from age-matched standardized control data in reading subtests in the DDE-2 battery (word list reading, pseudoword list reading, choosing the correct meaning of a word, search for misspellings of words; writing of word/pseudoword in

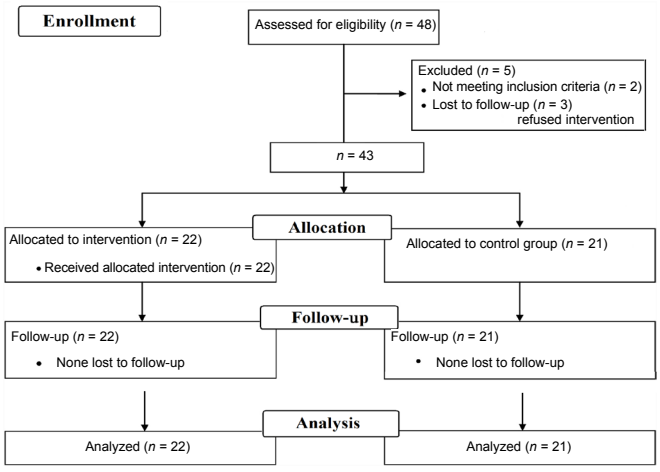

Figure 1 | **Participant flowchart diagram.**

dictation), as well as in the test battery "Reading abilities" (identifying the first sound in a heard word and omitted it in the word, fragmentation of the word in syllables and missed the last syllable, text reading, dictation of sentences filling in a missing compound word). In the control participants were included age-matched children with the same socio-demographical background as the dyslexic group, for who was no report of dyslexia or co-occurring language disorders confirmed by within-norm performance in speed and accuracy in reading. The results are shown in **Additional Table 1**.

Experimental paradigm

The participants were exposed to two types of visual stimuli, presented on a laptop with a screen resolution of 1920 × 1080 pixels and a refresh rate of 60 Hz at a distance of 57 cm from the observer. The stimuli stayed on the computer screen for 800 ms and consisted of words and pseudo-words, presented in pseudo-random order. The font used was Microsoft Sans Serif (black letters on a white background) and each letter had an angular size of about 1 degree. The words were selected according to their frequency of use, balancing common words with less common ones. The selected words were age-appropriate and encompassed the following parts of the speech: nouns, adjectives, verbs, numerals, prepositions, adverbs, pronouns, conjunctions. The pseudo-words were derived from the words by replacing all the vowels.

The stimuli were presented in two to four blocks during daily EEG experimental sessions, each block contained 40 words and 40 pseudo-words. Participants were asked to blink only during the interstimulus interval (1.5–2.5 seconds) to prevent artifacts in the EEG records during the words/pseudo-words stimuli. The participants were instructed to push a button with the right hand when seeing a word and to push a different button with the left hand when the stimulus was a pseudoword. Two behavioral parameters were evaluated for each child: the percentage of correctly identified words/pseudowords and the reaction time. In addition, to examine whether visual perceptional training can influence the neural semantic network of the dyslexic children, we recorded EEG session during visual word/pseudoword task one month later after training with five visual program interventions. Hence, irrespective of the word/pseudoword task, an intensive procedure with training tasks, presented in an arbitrary order and divided two-weekly in individual sessions of 45 minutes, was performed over a course of three months. This long term period does not enable the dyslexic children to memorize information about the word/pseudoword task, performed before the training period.

The visual perceptual training comprised five visual program interventions that do not include any direct phonological input on the dyslexic children. Such remediation programs were based on discrimination of directions in coherent motion stimuli, velocities in optic flow stimuli with a high-contrast texture. Discrimination of different low contrasts at high motion and low-spatial frequency sinusoidal gratings, embedded in external noise field, maximally activated magnocellular cells, as well as higher spatial frequency and higher levels of contrasts were used to increase parvocellular type activity and task complexity. In visual-spatial attentional task with high peripheral processing demands, either color change or color preservation of a square in a cue was identified in a briefly presented color array with four horizontally or vertically adjacent squares one of them in a black frame in either upper left or right visual field comparing with previous target array. Thresholds of parameters and program designs were described in previous works (Lalova et al., 2018, 2019) and literature (Wilmer et al., 2004; Benassi et al, 2010; Boets et al., 2011; Stein, 2014).

EEG recording and signal pre-processing

The EEG was recorded with an in-house developed 40-channel Wi-Fi EEG system using dry EEG sensors (each sensor is a matrix with 16 golden pins in a star-shaped configuration, Brain Rhythm Inc., Taiwan, China; Liao et al., 2011). Reference sensors were placed to both processi mastoidei and a ground sensor -on the forehead. The sensors were positioned on the head according to the international 10–20 system: F3, C3, T7, P3, O1; Fz, Cz, Pz, Oz; F4, C4, T8, P4, O2 and additional positions according to the 10-10 system: AF3, F7, FT9, FC3, FC5, C1, C5, CP1, CP3, TP7, P7, PO3, PO7, AF4, F8, FT10, FC4, FC6, C2, C6, CP2, CP4, TP8, P8, PO4, PO8. The skin impedance was controlled to be less than 5 kΩ. The sampling EEG rate was 250 Hz. The continuous EEG data was band-pass filtered into the following frequency bands: δ = 0.5–4; θ = 4–8; α = 8–13; β1 = 13–20; β2 = 20–30; γ1 = 30–48; γ2 = 52–70 Hz. The data was then segmented into trials, time-locked to the stimulus onset, each with a duration of 800 ms. Trials in which the EEG exceeded ± 200 μV were rejected as containing artifacts. Only trials with correct responses were included in the analysis.

Functional connectivity

The functional connectivity for all possible pairs of electrodes was determined using the Phase Lag Index (PLI) (Stam et al., 2007). This was done separately for each frequency band and trial. The PLI gives information about the phase synchronization of two signals, i.e. if one signal lags behind the other, by measuring the asymmetry of the distribution of their instantaneous phase differences. The instantaneous phases can be calculated from the analytical signal based on the Hilbert transform. The PLI can have values between 0 and 1. A value of 0 indicates that the two signals are not phase-locked (or that their phase difference is centered on 0 mod π), whereas a PLI of 1 means that they are perfectly phase-locked with a phase difference different from 0 mod π. PLI does not depend on the amplitude of the signal and is less sensitive to volume conduction in the brain, as well as spurious correlations because of common sources (Stam et al., 2007).

Minimum spanning tree

The calculated connectivities, using the PLI, between each pair of channels can be used to construct an adjacency matrix, i.e., a graph. Due to methodological limitations, the comparison of different brain networks can be problematic (Fornito et al., 2010; van Wijk et al., 2010; Tewarie et al., 2015). To avoid this problem, some authors have proposed the use of the minimum spanning tree (MST) (Tewarie et al., 2015) to define an unbiased subgraph of the original network. A separate MST sub-graph was constructed from each of the PLI matrices, i.e. one for each non-rejected trial.

The MST is a unique sub-graph, that connects all the nodes of the graph without forming loops, such that the wiring cost (the weights) is minimized. The MST was constructed using Kruskal's algorithm (Kruskal, 1956). Since we were interested in the strongest connections, before using the algorithm all the original weights (PLI) were converted to distances (1/PLI). The first step of the procedure is to order all the links in ascending order. After that, the link with the shortest distance (highest PLI) is added to the sub-network. Next, the link with the second shortest distance, which does not form any loops, is added and this procedure is repeated until all the nodes are connected in an acyclic graph. In the end, all the links present in the MST are set to 1, while all the other connections are set to 0, i.e., the MST is a binary graph. The MST has a fixed density – M = N – 1, where N is the number of nodes. There are two extreme MST topologies: (1) line-like topology, in which each node is connected to only two other nodes, with the exception of the two leaf nodes at either end of the line; (2) star-like topology, in which there is a single central node to which all the other nodes are directly connected. The MST captures most of the properties of a complex network in an unbiased subnetwork, but due to the acyclicity, the resultant networks have lower density, which may lead to a loss of information about the original network (Smith et al., 2017). The tree's topology can be characterized by various measures (Boersma et al., 2013). The global MST measures, like conventional graph measures, can provide information about network integration and segregation (Tewarie et al., 2015). Four global MST measures were used in this study: diameter, leaf fraction, tree hierarchy and kappa. The diameter in the MST is the shortest path along the minimum spanning tree. The shortest path between two nodes in the network is the path that involves the fewest number of links between them. Leaf fraction is the number of leaves (nodes with degree = 1) in the MST divided by the total number of nodes. The tree hierarchy (Boersma et al., 2013) is a metric that characterizes the balance of having high network integration without overloading the most important nodes in the network. The tree hierarchy is defined as $TH = L/2mBC_{max}$, where m = N – 1 links in the MST, N is the number of nodes, L is the number of leaves and BCmax is the maximal betweenness centrality (BC) in the MST. TH has values between 0 and 1. On one extreme if the tree has a line-like topology, i.e., L = 2, then if m approaches infinity, TH will approach 0. On the other end, if the tree is star-like, L = m and TH approaches 0.5. For topologies between these two extreme cases, TH will have higher values. Kappa measures the broadness of the degree distribution in the network (Barrat et al., 2008) and has higher values for scale-free graphs and lower values for more random graphs. Kappa reflects the resilience of the network against attacks related to targeted hub removal, specifically a change in the degrees of the connected nodes. High kappa means the network is less vulnerable to random attacks. All these global MST measures were calculated separately for each non-rejected trial.

The nodal measures give information about the importance of individual nodes in the network. Two measures of nodal centrality were used in the subsequent analyses: degree and BC. The degree of a node is equal to the number of nodes it's connected to. Betweenness centrality of a node is the fraction of all shortest paths in the network that pass through that node. Nodes with a high degree or a high betweenness centrality play an important part in information processing in the network (Boccaletti et al., 2006). The networks are more integrated when they have a higher maximum degree or maximum betweenness centrality (Bullmore and Sporns, 2009; Stam et al., 2014).

The MST analysis was performed using the Brain Connectivity Toolbox for Matlab (Rubinov and Sporns, 2010; Vanderbilt University, Nashville, Tennessee, USA; MathWorks Inc., Natick, MA, USA). For the visualization of the hubs on a group level, the local MST measures (degree, BC) were first averaged across all the non-rejected trials for each subject. The obtained subject-level degree/BC were then averaged across subjects to obtain the group-level local measures. The hubs were calculated from these group averaged degree/BC values. Hubs were defined to be nodes with degree/BC of at least 1 standard deviation above the mean and are presented in red color on the figures. The links on the figures represent the most important links with edge BC (obtained from the group average) of at least 1 standard deviation above the mean. All the figures were generated using BrainNet Viewer version 1.63 (Xia et al., 2013; Beijing Normal University, China).

Statistical analysis

In EEG recording sessions, the reaction times and performance accuracy of pre- and post-training dyslexic subgroups were compared for each condition (words/pseudowords), as well as those of dyslexics and neurotypical readers by a Kruskal Wallis nonparametric test (KW test; Matlab kruskal wallis function). All statistical analysis was performed using Matlab Statistics toolbox 2013 (MathWorks Inc., Natick, MA, USA).

For each frequency band, the global MST measures and the hubs, determined by the local measures degree and BC, were compared between groups using nonparametric Kruskal-Wallis tests (K-W test). The indices of the sensors were chosen so that the statistical tests for hubs were most sensitive to hemispheric differences. The comparisons were made using the measures from all the non-rejected trials of all the subjects of the specific group. To compensate for the effects of multiple comparisons, a Bonferroni correction to the significance level was applied separately for the global tests ($P = \alpha/4 = 0.0125$) and the local (hubs) tests ($P = \alpha/2 = 0.025$). All the *P*-values that showed significant results (< the Bonferroni corrected significance level) are presented in bold text.

Results

Behavioral results

The results of the between-group comparisons (K-W test) of the behavioral measures (percentage of correct answers and reaction time) are shown in **Table 1**. Both dyslexic groups (before training and after training) showed a lower success rate and slower reaction times compared to the controls in both conditions (words and pseudowords). After training the dyslexics showed an improvement in the percentage of correct answers ($\chi^2 = 4.51$, $P < 0.03$ for words; $\chi^2 = 5.29$, $P = 0.02$ for pseudowords), their reaction times however did not change significantly.

Global MST measures

Statistically significant differences were found between the global MST measures of the controls and those of the pre-training dyslexic group. The smaller diameter and the bigger leaf fraction that the networks of the dyslexics have in most of the frequency bands are characteristic of a more integrated star-like topology (**Tables 2** and **3**). On the other hand, the bigger diameter and the smaller leaf fraction, shown by the controls are indicative of a more segregated topology (**Tables 2** and **3**). MST networks with smaller diameters tend to have higher tree hierarchy and higher kappa (He et al., 2019).

Significant differences in all of the four global MST measures were found between the controls and the pre-training dyslexic group in the θ, β, and γ frequency bands for the word condition (**Table 2**) and in γ for the pseudo-words (**Table 3**). Compared to the controls, the pre-training dyslexics had higher leaf fraction, tree hierarchy and kappa, and lower diameter ($P < 0.01$, **Table 2**). The lower diameter (for θ: $\chi^2 = 18.07$, $P < 0.0001$) and the higher leaf fraction (for θ: $\chi^2 = 18.52$, $P < 0.0001$) of the pre-training dyslexic group suggest a

Table 1 | **Nonparametric statistical comparison of the behavioral parameters**

Visual discrimination task	Controls	Pre-training Dys	Post-training Dys	Pre-training Dys *vs*. Con		Post-training Dys *vs*. Con		Pre-training *vs*. Post-training Dys	
				χ^2	*P*	χ^2	*P*	χ^2	*P*
Word									
Success rate (%)	94.66±1.15	69.83±2.75	78.6±2.99	28.5	**< 0.0001**	19.2	**< 0.0001**	4.51	**0.03**
RT time (ms)	1149.1±13.28	1333.8±18.52	1369.3±19.82	61.8	**< 0.0001**	91.2	**< 0.0001**	2.87	0.08
Pseudoword									
Success rate (%)	91.7±1.52	55.58±3.71	69.5±5.04	32.4	**< 0.0001**	13.05	**0.0003**	5.29	**0.02**
RT time (ms)	1313.4±15.21	1543.3±22.6	1537.8±22.2	73.7	**< 0.0001**	89.1	**< 0.0001**	0.07	0.70

Data are expressed as the mean ± SE. Bold font indicates statistically significant effects. Dys: Dyslexic children; RT: reaction time.

Table 2 | **Nonparametric statistical comparison of the global metrics of the brain networks of controls, pre-training and post-training dyslexic groups during discrimination of words**

Metrics		Controls	Pre-training Dys	Post-training Dys	Con *vs* Pre-training Dys		Con *vs* Post-training Dys		Pre-training *vs* Post-training Dys	
					χ^2	*P*	χ^2	*P*	χ^2	*P*
δ	D	0.286±0.005	0.279±0.005	0.263±0.006	0.19	0.667	8.33	**0.004**	5.2	0.02
	LF	0.597±0.006	0.614±0.008	0.624±0.009	1.54	0.215	6.37	**0.012**	1.7	0.19
	TH	0.416±0.005	0.427±0.005	0.422±0.006	2.09	0.149	0.86	0.354	0.1	0.70
	K	3.663±0.079	3.954±0.152	4.039±0.151	0.02	0.893	2.83	0.093	1.9	0.16
θ	D	0.334±0.004	0.309±0.004	0.329±0.004	18.07	**< 0.0001**	0.81	0.368	9.9	**0.0017**
	LF	0.541±0.004	0.572±0.005	0.545±0.005	18.52	**< 0.0001**	0.49	0.481	11.3	**0.0008**
	TH	0.402±0.004	0.416±0.004	0.404±0.004	6.78	**0.009**	0.12	0.732	4.7	0.0297
	K	3.071±0.035	3.384±0.057	3.087±0.044	23.17	**< 0.0001**	0.08	0.781	18.8	**< 0.0001**
α	D	0.324±0.003	0.318±0.003	0.327±0.004	1.66	0.198	0.50	0.479	3.7	0.05
	LF	0.535±0.004	0.554±0.004	0.535±0.004	9.83	**0.002**	0.001	0.974	10.1	**0.0015**
	TH	0.396±0.003	0.405±0.003	0.394±0.003	4.05	0.044	0.005	0.943	3.6	0.057
	K	3.025±0.027	3.168±0.035	3.009±0.027	9.88	**0.002**	0.0002	0.988	9.6	**0.0019**
β1	D	0.330±0.003	0.315±0.003	0.325±0.004	10.62	**0.001**	2.47	0.116	2.1	0.14
	LF	0.518±0.003	0.548±0.004	0.517±0.004	28.30	**< 0.0001**	0.05	0.829	26.9	**< 0.0001**
	TH	0.383±0.003	0.398±0.003	0.381±0.003	10.96	**0.0009**	0.15	0.701	11.6	**0.0006**
	K	2.941±0.027	3.081±0.028	2.906±0.021	25.19	**< 0.0001**	0.006	0.938	23.1	**< 0.0001**
β2	D	0.328±0.003	0.313±0.003	0.325±0.003	12.50	**0.0004**	0.69	0.403	6.1	0.0136
	LF	0.523±0.003	0.546±0.004	0.517±0.004	19.54	**< 0.0001**	1.96	0.162	29.5	**< 0.0001**
	TH	0.388±0.003	0.399±0.003	0.383±0.003	9.82	**0.0017**	1.23	0.267	15.2	**< 0.0001**
	K	2.913±0.020	3.083±0.029	2.884 ±0.021	25.77	**< 0.0001**	0.74	0.391	30.8	**< 0.0001**
γ1	D	0.323±0.003	0.302±0.003	0.316±0.003	16.78	**< 0.0001**	1.06	0.303	9.6	**0.0019**
	LF	0.530±0.004	0.560±0.004	0.535±0.004	27.22	**< 0.0001**	0.89	0.347	19.9	**< 0.0001**
	TH	0.388±0.003	0.404±0.003	0.390±0.003	14.82	**< 0.0001**	0.17	0.677	11.6	**0.0006**
	K	2.990±0.025	3.184±0.031	2.994±0.029	28.20	**< 0.0001**	0.60	0.437	20	**< 0.0001**
γ2	D	0.277±0.002	0.262±0.003	0.271±0.003	18.97	**<0.0001**	3.07	0.079	5.97	0.0145
	LF	0.595±0.003	0.632±0.004	0.612±0.004	45.26	**< 0.0001**	8.97	0.003	12.2	**0.0005**
	TH	0.418±0.003	0.434±0.003	0.427±0.003	16.99	**< 0.0001**	3.61	0.057	3.9	0.048
	K	3.408±0.034	3.881±0.060	3.575±0.041	53.16	**< 0.0001**	11.58	**0.001**	12.5	**0.0004**

The significant level for the global metrics after Bonferroni correction is *P* = 0.0125. Bold font indicates statistically significant effects. Frequency bands (Hz): δ = 0.5–4; θ = 4–8; α = 8–13; β1 = 13–20; β2 = 20–30; γ1 = 30–48; γ2 = 52–70 Hz. Data are expressed as the mean ± SE. D: Diameter; Dys: dyslexic children; K: kappa; LF: leaf fraction; TH: tree hierarchy.

more integrated network compared to the controls. The pre-training dyslexics also had a higher tree hierarchy compared to the controls (θ: *P* = 0.009; β1: *P* = 0.001; β2: *P* = 0.002; γ1, γ2: *P* < 0.0001). The tree hierarchy reflects how optimal is the configuration of the MST, i.e. an efficient communication without overloading hubs. The higher tree hierarchy and the higher leaf fraction found in the dyslexics before training point to a more loaded neural network compared to the controls. After a remedial training, the global MST measures revealed that in most frequency bands the network topology of the dyslexic children had become more segregated and similar to the topology of the controls. The exceptions were the higher leaf fraction in δ (*P* = 0.012) and in γ2 (*P* = 0.003; words), the higher kappa in γ2 (*P* = 0.001, words; *P* = 0.004, pseudowords) and the lower diameter in δ (*P* = 0.004, words; **Tables 2** and **3**).

In the θ band, the leaf fraction and kappa decreased after training, and the diameter increased (*P* = 0.0017, *P* = 0.0008, *P* < 0.0001; **Table 2**), which indicates that the topology had become more segregated compared to the one before training. In the α and γ2 bands, the leaf fraction and kappa also decreased after training (*P* < 0.0015; **Tables 2** and **3**), however in γ2 their values still remained significantly higher than the ones of the controls. The tendency of the leaf fraction, kappa and tree hierarchy to decrease after training (*P* < 0.0006; **Tables 2** and **3**) was also present in the β1, β2 and γ1 frequency bands. In the γ1 (for both conditions) and in the β2 (for pseudowords) band, the post-training dyslexic group also showed a significant increase in the diameter (*vs*. before training) (*P* < 0.005, **Tables 2** and **3**; in β2, *P* = 0.003, **Table 3**).

Distribution of connectivity hubs

For the word condition, the between-group comparisons

Table 3 | **Nonparametric statistical comparison of the global metrics of the brain networks of control, pre-training and post-training dyslexic groups during pseudo-word discrimination**

					Con *vs.* Pre-training Dys		Con *vs.* Post-training Dys		Pre-training *vs.* Post-training Dys	
Metrics		Controls	Pre-training Dys	Post-training Dys	χ^2	*P*	χ^2	*P*	χ^2	*P*
δ	D	0.278±0.005	0.285±0.005	0.274±0.007	0.20	0.654	0.74	0.391	1.6	0.2
	LF	0.597±0.006	0.603±0.006	0.612±0.009	0.40	0.526	2.45	0.117	0.75	0.39
	TH	0.414±0.005	0.428±0.004	0.426±0.006	4.09	0.043	1.77	0.183	0.12	0.73
	K	3.638±0.081	3.502±0.064	3.720±0.104	1.44	0.230	0.33	0.567	3.1	0.08
θ	D	0.328±0.008	0.323±0.005	0.325±0.005	0.55	0.459	0.19	0.659	0.05	0.8
	LF	0.546±0.004	0.556±0.005	0.544±0.005	0.74	0.390	0.09	0.763	1.1	0.3
	TH	0.401±0.003	0.411±0.004	0.402±0.004	2.68	0.101	0.001	0.979	2.27	0.13
	K	3.106±0.033	3.236±0.056	3.159±0.049	1.29	0.255	0.06	0.807	1.6	0.21
α	D	0.328±0.003	0.320±0.004	0.328±0.007	1.72	0.189	0.004	0.947	1.5	0.22
	LF	0.534±0.004	0.547±0.005	0.526±0.004	3.83	0.050	1.67	0.197	9.2	**0.002**
	TH	0.393±0.003	0.399±0.004	0.387±0.004	1.11	0.292	2.32	0.128	5.6	0.017
	K	3.004±0.028	3.147±0.043	2.969±0.028	6.88	**0.009**	0.21	0.647	8.9	**0.0029**
β1	D	0.332±0.003	0.318±0.003	0.327±0.004	8.22	**0.004**	0.48	0.488	3.9	0.047
	LF	0.519±0.003	0.538±0.004	0.518±0.004	12.17	**0.0005**	0.17	0.677	13.2	**0.0003**
	TH	0.384±0.007	0.393±0.003	0.381±0.003	3.13	0.076	1.36	0.244	6.8	**0.009**
	K	2.911±0.020	3.047±0.030	2.912±0.026	18.03	**< 0.0001**	0.05	0.817	17.6	**< 0.0001**
β2	D	0.327±0.003	0.316±0.003	0.331±0.003	1.77	0.183	3.24	0.072	9.1	**0.003**
	LF	0.517±0.0060	0.539±0.004	0.512±0.004	11.91	**0.0006**	1.81	0.179	21.1	**< 0.0001**
	TH	0.380±0.003	0.394±0.003	0.379±0.004	8.96	**0.0028**	0.34	0.557	10.5	**0.001**
	K	2.907±0.021	3.064±0.03	2.870±0.022	21.60	**< 0.0001**	0.96	0.327	29	**< 0.0001**
γ1	D	0.323±0.003	0.307±0.003	0.320±0.003	13.10	**0.0003**	0.47	0.494	7.8	**0.005**
	LF	0.528±0.004	0.562±0.004	0.532±0.004	39.08	**< 0.0001**	1.95	0.163	20.5	**< 0.0001**
	TH	0.386±0.003	0.407±0.003	0.391±0.003	21.34	**< 0.0001**	1.90	0.168	10.1	**0.001**
	K	2.947±0.026	3.231±0.037	2.976±0.025	53.53	**< 0.0001**	2.91	0.088	29.4	**< 0.0001**
γ2	D	0.275±0.002	0.264±0.003	0.272±0.003	8.34	**0.004**	0.98	0.322	2.8	0.09
	LF	0.605±0.003	0.635±0.004	0.616±0.005	29.61	**< 0.0001**	4.88	0.027	6.6	**0.011**
	TH	0.430±0.003	0.447±0.003	0.430±0.004	13.74	**0.0002**	0.01	0.911	9.9	**0.002**
	K	3.448±0.038	3.818±0.057	3.646±0.052	36.66	**< 0.0001**	8.22	0.004	6.4	**0.011**

The significant level for the global metrics after Bonferroni correction is *P* = 0.0125. Bold font indicates statistically significant effects. Frequency bands (Hz): δ = 0.5–4; θ = 4–8; α = 8–13; β1 = 13–20; β2 = 20–30; γ1 = 30–48; γ2 = 52–70 Hz. Data are expressed as the mean ± SE. D: Diameter; Dys: dyslexics; K: kappa; LF: leaf fraction; TH: tree hierarchy.

in the δ-band, did not show significant differences in hub distributions, based on the degree of the nodes, between the controls and pre-training dyslexic group (χ^2 = 2.08, *P* = 0.149) and between the controls and post-training dyslexics (χ^2 = 2.16, *P* = 0.141; **Additional Table 2**). There was, however, a statistically significant difference between the hub distributions of the pre-training and post-training dyslexic group (χ^2 = 6.7, *P* = 0.009). The hubs for the normally reading children were located in the left superior frontal gyrus (SFG; Fz covers BA6 – premotor cortex; sensor AF3: BA9 – dorsolateral prefrontal cortex; Koessler et al., 2009), the left middle frontal gyrus (MFG; F3: BA8 – intermediate frontal cortex), the left inferior frontal gyrus (IFG; F7: BA45/47 – Broca's area, orbital frontal cortex), the left inferior temporal gyrus (ITG; FT9: BA20 – inferior temporal gyrus, Koessler et al., 2009; BA38 – temporal pole, Giacometti et al., 2014) and in the left precentral gyrus (PreCG; Cz, C1: BA4, BA6 – primary motor, premotor and supplementary motor cortices). The hubs in pre-training children with DD were in the bilateral SFG (AF3, AF4) and the left IFG (F7). After training, in addition to hubs in the left SFG (AF3) and the left IFG (F7), there were also hubs that had not appeared in the network of the same group before training: in the left MFG (F3), the left ITG (FT9) and the left postcentral gyrus (PstCG; C5: BA123, BA40 – primary somatosensory cortex, supramarginal gyrus). The statistical comparison between the two dyslexic groups also revealed that after training, the dyslexics had more hubs in the left hemisphere.

Unlike the results for the δ-band, in the θ-band, there was a significant difference in the distribution of hubs (degree) between the controls and the pre-training dyslexic group (χ^2 = 9.29, *P* = 0.002; **Additional Table 2**; **Figure 2A**, 1st plot). For the control group, the hubs were located in the SFC (Fz), the bilateral ITG (FT9-10) and the right middle occipital gyrus (MOG; PO8: BA18- secondary visual cortex and inferior occipital gyrus; Giacometti et al., 2014). For the pre-training dyslexic group, the hubs were located in the SFC (Fz, AF3), the right MFG (F4), the left IFG (F7), the right PreCG (C2), the right MOG (PO8: BA18; O2: BA18) and the left middle temporal gyrus (MTG; T7: BA21; **Figure 2A**, 2nd plot). The differences in the networks of the two groups were due to the controls having more hubs in the anterior part of the left hemisphere, whereas the pre-training dyslexics had more hubs in the posterior part in the right hemisphere. The between-group hub distribution comparison (degree) between controls and post-training children with DD showed no statistical difference (θ-band: χ^2 = 1.26, *P* = 0.262). There was no statistical difference between the two dyslexic groups (χ^2 = 3.5, *P* = 0.06). After training the hubs were located entirely in the left hemisphere in the SFG (AF3, Fz), the MFG (F3), the ITG (FT9), MTG (T7), the PreCG (Cz), the PstCG (C5; C3: BA123) and a part of the cuneus of the occipital lobe (Oz: BA18; **Figure 2A**, 3rd plot).

The between-group comparisons of the hubs (degree), also revealed a statistically significant difference between controls and the pre-training dyslexics in the α-band (χ^2 = 5.26, *P* = 0.022), with the dyslexic children showing more hubs in the posterior part of the right hemisphere. Controls' hubs were located in the SFG (Fz), the left ITG (FT9), the left PreCG (C1, Cz), the left PstCG (C5), the right MOG (PO8, O2) and the cuneus (Oz; **Figure 2B**, 1st plot). For the pre-training dyslexic group, the hubs were in the SFC (Fz), the left MFG (FC3), the right PreCG (C2), the right superior occipital gyrus (SOG, PO4:

BA19 – associative visual cortex), the bilateral MOG (P07–O8) and the cuneus (Oz; **Figure 2B**, 2nd plot). After training, the hubs were located in the SFG (Fz), the left ITG (FT9), the left PreCG (C1), the right ITG (P8: BA37), the right SOG (PO4), MOG (PO8, O2) and the cuneus (Oz; **Figure 2B**, 3rd plot). The KW tests did not show significant differences between controls and the post-training dyslexic group (χ^2 = 2.98, P = 0.084; **Additional Table 2**). There wasn't a significant difference between the two dyslexic groups either (χ^2 = 0.2, P = 0.66).

The hub distributions, based on the BC of nodes, differed between controls and the pre-training dyslexic group in the β1-band (χ^2 = 4.9, P = 0.022; **Figure 2C**; **Additional Table 2**) because the hub distribution of the pre-training dyslexics was shifted more towards the right hemisphere compared to the control group. For the controls, hubs were located in the left MFG (F3), the left ITG (FT9), the left PstCG (C3, C5) and the left ITG (P7: BA37) (**Figure 2C**, 1st plot), whereas for the pre-training dyslexic group, the hubs were in the bilateral SFG (AF3–4), the bilateral MFG (F3–4), the left ITG (FT9), the bilateral PreCG (C1–2), the right ITG (P8) and the right MOG (PO8; **Figure 2C**, 2nd plot). For the post-training dyslexic group, the hubs were in the left SFG (AF3, Fz), left PstCG (C5), the left superior parietal lobe (SPL; CP1: BA7, BA5) and the right MOG (PO8, O2). The difference between the controls and the post-training dyslexic group was not significant (χ^2 = 0.25, P = 0.614).

For the pseudoword condition, in the δ-band, the between-group comparisons for the hubs (degree) revealed significant differences between controls and the pre-training dyslexic group (χ^2 = 10.02, P = 0.002; **Additional Table 3**), with the controls having more hubs in the anterior part of the left hemisphere. Since the main hubs of both dyslexic subgroups were in left SFG (AF3), left MFG (FC3), left IFG (F7) and left ITL (FT9), the significant differences (χ^2 = 9.00, P = 0.0028) were due to the pre-training group having more hubs in the right hemisphere. There was no significant difference in hub distribution between the controls and the post-training dyslexic group (χ^2 = 0.03, P = 0.854; **Additional Table 3**).

In the δ-band, the hubs (BC) of the pre-training dyslexic group were in bilateral SFG (AF3-4), left MFG (FC3), left IFG (F7), left ITL (FT9), after training the hubs were located in the left SFG (AF3), the left MFG (FC3, F3), the IFG (F7), the left ITL (FT9) and the right MOG (O2). There was a statistical difference between the hub distributions of the dyslexic groups (χ^2 = 6.8, P = 0.0089; **Additional Table 3**). The post-training group had more hubs in the anterior part of the left hemisphere.

For the β1-band (pseudoword condition), the hub distributions of the control and the pre-training dyslexic groups, based on the BC metric, were significantly different (χ^2 = 9.13, P = 0.003; **Additional Table 3**), because the dyslexics had fewer hubs in the left hemisphere. The hubs for the controls were located in the left SFG (AF3, Fz), the left ITL (FT9), the left PreCG (C1) and the right PstCG (C6; **Figure 2D**, 1st plot). For the pre-training dyslexic group, the hubs were in the left SFG (AF3), the right ITL (FT10), the right MTG (T8), the PstCG (Cz), the right PreCG (C2), the right PstCG (CP2: BA5, 7), the right inferior parietal lobe (IPL, P4: BA39, 7, 40, 19) and the left MOG (PO7; **Figure 2D**, 2nd plot), whereas after training the hubs were in the bilateral IFG (F7-8), the right PstCG (C4) and the right MOG (PO8; **Figure 2D**, 3rd plot). The statistical tests did not reveal any significant differences between the hub distributions of the controls and the post-training dyslexic group (χ^2 = 0.22, P = 0.614). Compared to the pre-training dyslexic group, the hub distribution of the post-training group contained more hubs in the anterior part of the left hemisphere (χ^2 = 5.6, P = 0.018).

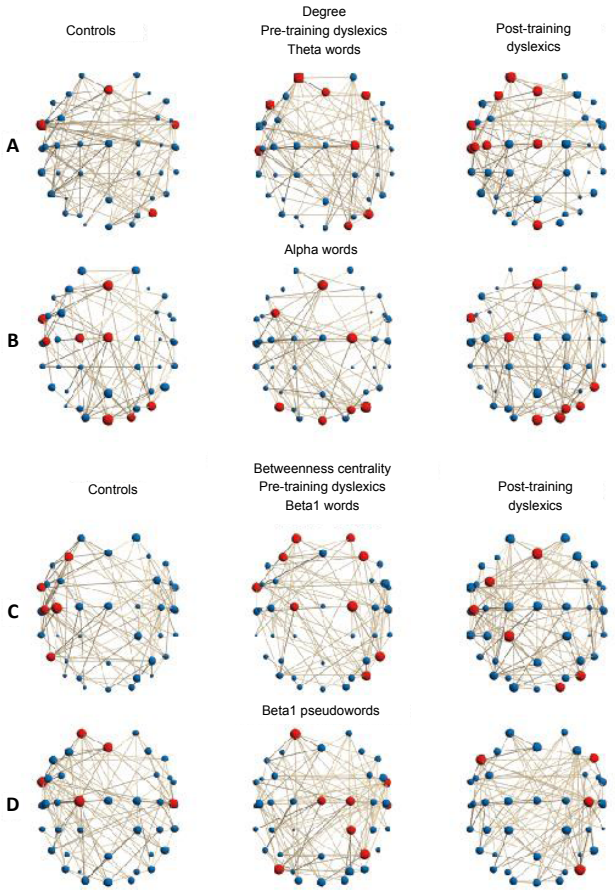

Figure 2 | Visualization of the hubs on a group level for selected frequency bands.

Each node corresponds to an EEG sensor. The hubs, presented in red color, were obtained from the group averaged degree/BC values and were defined to be nodes of at least 1 standard deviation above the mean. The links on the figures represent the most important links with edge BC (obtained from the group average) of at least 1 standard deviation above the mean: (A, graph 1) Hubs (degree) in the theta band for the word condition for controls: FT9, FT10, Fz, PO8; (A, graph 2) for pre-training dyslexics: AF3, F7, Fz, F4, T7, C2, PO8, O2; (A, graph 3) for post-training dyslexics: AF3, F3, FT9, Fz, T7, Cz, C3, C5, Oz. (B, graph 1) Hubs (degree) in the alpha band for the word condition for controls: Fz, FT9, C5, Cz, C1, PO8, O2, Oz; (B, graph 2) for pre-training dyslexics Fz, FC3, C2, PO4, PO8, PO7, Oz; (B, graph 3) for post-training dyslexics Fz, FT9, C1, P8, PO4, PO8, Oz, O2. (C, graph 1) Hubs (BC) in the beta1 band for the word condition for controls: FT9, F3, C3, C5, P7; (C, graph 2) for pre-training dyslexics AF3, AF4, FT9, F3, F4, C1, C2, PO8, P8; (C, graph 3) for post-training group FC3, Fz, C5, CP1, PO8, O2. (D, graph 1) Hubs (BC) in the beta1 band for the pseudoword condition for controls: AF3, FT9, Fz, C1, C6; (D, graph 2) for pre-training dyslexics AF3, FT10, Cz, C2, CP2, T8, P4, PO7; (D, graph 3) for post-training dyslexics F7, F8, C4, PO8.

Discussion

Aberrant global topology in dyslexia

This study used a graph analytical approach based on the MST, to investigate the topology of the functional brain networks, derived from EEG data, of controls and dyslexic children during the performance of a visual word/pseudoword discrimination task. The results suggest that before training dyslexic children exhibit a different global topological organization compared to the controls, and that with training their global topology becomes more similar to that of the controls.

A recent MRI study investigating the resting state structural brain networks of Chinese dyslexics revealed that the dyslexic children, compared to the controls, had an altered topological organization with increased local efficiency and decreased global efficiency (Liu et al., 2015).

The MST diameter is highest for regular networks and decreases as the networks become more random. The leaf fraction, on the other hand, is lowest for regular networks and increases as the networks become more random. The diameter

and the leaf fraction have extreme values for scale-free networks, i.e., the diameter is lowest, and the leaf fraction is highest in a scale-free network (Tewarie et al., 2015). The smaller diameter and the higher leaf fraction that pre-training dyslexic children showed in most of the frequency bands, is indicative of a more integrated star-like topology compared to the controls that showed a more decentralized network. These findings show that, compared to typically developing children, dyslexics exhibited a different global brain topology during the performance of a visual task, however, the between-group differences in MST measures are in contrast to the previously reported differences in networks at rest (Fraga González et al., 2016).

An efficient network would be one that optimally balances between local processing and global integration. The more integrated network of pre-training dyslexics could reflect a less optimal global organization with overloading of central connectivity hubs. The change in network topology after training could be the result of a compensatory mechanism.

The higher diameter and the lower leaf fraction, tree hierarchy and kappa found in the control group, compared to the pre-training dyslexics, could reflect a more mature brain. After training, the changes in the MST measures of dyslexic children were similar to the changes observed in the process of brain maturation (He et al., 2019). The increase of topological segregation after training decreases the load on the important, in terms of connectivity, brain regions, leading to a more efficient brain network, analogous to the processes observed in the brain development of children (Hagmann et al., 2010). The between-group differences in MST measures were mostly frequency-independent. They had a similar profile in most of the bands, suggesting that similar network constraints occur in different neural circuits. Significant correlations have been found between network indices and phonological decoding ability in the 8–13 Hz and 20–30 Hz EEG bands (Vourkas et al., 2011). The idea that dyslexics may exhibit differences in brain connectivity would be consistent with the evidence and theoretical models suggesting deficits in general sensory functions and attention that are associated with higher frequency EEG activity (alpha and beta).

Our results revealed that, compared to typically developing children, dyslexic children exhibit a different topological organization of their brain networks and that with training, these networks reorganize and become more segregated. These changes after training are similar to the changes observed in brain maturation, in which the smaller diameter and the higher leaf fraction that children have, compared to adults, indicate that the topology of the functional brain networks becomes less centralized with development (He et al., 2019). The lower tree hierarchy and kappa after training also indicate a better-balanced network with a lower risk of an overload of its most important regions.

Changes in the segregation of brain functional systems during brain development are related to improving the brain network organization, characterized by increasing segregation between the functional systems of the brain regions, and increasing the specialization of their functions. Reduced segregation of task-related brain systems of dyslexics before training that accompanies new performance tasks subside with continued practice, leading to automation of some tasks and provides further evidence that segregation of large-scale systems shows dynamic changes in relation to the requirements for processing in the more short term periods.

Increasing segregation in the brain systems of typical children is associated with a high cognitive ability as good long-term episodic memory. The relationship between systemic segregation and cognitive ability sustains independently of age throughout life. Brain networks, which have segregated systems, are flexible to certain types of interference. A brain disorder, especially caused in crucial hub locations, is associated with increased functional connectivity between the systems or reduced segregation. Dyslexics who have undergone cognitive remedy training provide additional support necessary for systematic segregation to promote cognition. Post-trained dyslexics with a higher level of segregation than before training may beneficially change cognition with training. Overall, the results in the group of post-trained dyslexics have provided guidance in understanding the mechanisms by which systemic segregation may be altered.

Regional topological changes of hubs

The brain regions showing between-group differences in the presence of hubs were different for the different frequency bands.

Delta frequency activity during the performance of mental tasks correlates with task proficiency (Vogel et al., 1968; Harmony, 2013). During semantic tasks, delta activity in the frontal attention networks plays an important role in inhibiting the activity of other networks that may interfere with the performance of the task (Harmony, 2013). In the delta frequency band, during the word discrimination condition, before training the dyslexics showed hubs in the bilateral intermediate frontal cortices and the inferior frontal cortex, however after training hubs were located in regions responsible for the focusing of attention, i.e., in the left intermediate frontal, the dorsolateral prefrontal and the inferior frontal gyrus, as well as hubs in the left anterior regions of the temporal lobe, left primary and secondary somatosensory cortices, which are responsible for perceptual specialization. For the pseudoword condition, unlike the pre-training dyslexics, both the controls and the post-training dyslexics showed delta hubs (BC) located in the frontoparietal network- lateral prefrontal cortex, postcentral gyrus, portion of inferior parietal lobe, middle temporal lobe, associative and secondary visual cortices, and occipitotemporal cortex – which is responsible not only for perceptual specialization but for cognitive control and decision-making (Vincent et al., 2008). For both controls and the post-training dyslexic group, these inhibitory delta oscillations, originating in the frontal cortex (Harmony, 2013), are better able to modulate the activity of other neural networks, thus facilitating the focusing of attention on the task.

In the theta and beta1 frequency bands, we observed between-group differences in the appearance of hubs in the left superior and middle frontal cortices, and in the posterior semantic network- inferior parietal lobe (postcentral and supramarginal gyri), inferior temporal lobe, and occipitotemporal cortex. Previous studies have found atypical lateralization of theta and beta rhythms in dyslexics during the performance of language tasks (Spironelli et al., 2008). During the word condition, the hubs in the anterior temporal lobes (θ, α), the inferior parietal lobe (α, β1), and around the middle temporal gyrus (β1) were almost absent in the left hemisphere of the pre-training dyslexic group. For the pseudoword condition, the controls and the post-training dyslexics showed hubs in the anterior temporal lobes (including the anterior part of the inferior, middle and superior temporal gyri; β1 band), not present in the pre-training group. This means that the remediation training can have an effect on the temporal-parietal network of the left hemisphere of the dyslexic group. Compared to the pre-training group, the post-training group showed more hubs in the left medial prefrontal cortex (θ frequencies), the left anterior temporal lobe (θ, α), the left somatosensory cortex (θ, α, β1; word condition) and the left inferior frontal gyrus (β1, pseudoword condition).

Hubs in the left frontal-temporal areas identified in the

network of typically developing children were not presented in the brains of pre-training children with DD (θ, α and β1 frequencies). Higher accuracy of task performance after training and specific connectivity hubs in posterior regions (left preparietal and superior parietal cortices in β band) suggest that alternative neural pathways exist in dyslexics to compensate for deficient neuronal processing during task performance (Wolf et al., 2010). The results show that the left anterior temporal lobe, the postcentral gyrus and the inferior parietal lobe have a significant role in visual word discrimination and are important hubs for the functional network of the controls. The appearance of hubs for controls (θ band), as a result of the pseudoword presentation, in the left anterior temporal lobe is accompanied by hubs in the right anterior temporal lobe and the superior frontal gyrus. The presence of hubs in the left anterior temporal and superior temporal lobes together with hubs in the sensorimotor regions (β1 frequency) could explain the faster reaction times of the controls compared to the two dyslexic groups. In the beta1 band, during the word discrimination condition, the hubs of the controls were located in the left inferior parietal lobe and in the left somatosensory cortex, whereas for the pseudoword condition, the hubs were in the left anterior temporal lobe and in the left orbitofrontal cortex. On the other hand, the hubs of the dyslexic pre-training group were located in the right inferior parietal lobe and in the right somatosensory cortex for the word condition, and in the right anterior temporal lobe and in the left orbitofrontal cortex for the pseudoword condition. After training, the dyslexic children had hubs in the left inferior parietal lobe and in the left orbitofrontal cortex for the word condition (**Additional Table 3**, beta1), and in the left inferior frontal and the right somatosensory cortices for the pseudoword condition. We suppose that in dyslexic children, the hubs coordinating the heteromodal semantic network and the hubs in the sensory regions are located in the right hemisphere, instead of the left one.

Although participants' lexical decisions may be due to the expectation of words that they have already built up through their word experience at least to some extent prior to the experiment, they could not build up such an expectation for pseudowords before actually seeing them. The decision criteria used by dyslexics in the earlier experiment may be different from those used later in the pseudo-word condition. However, for both conditions, the dyslexics' inverted lateralization on anterior regions before training in comparison to those after remediation training, suggests functional impairment of a main linguistic center as the left frontal cortex. It also has been suggested that certain brain areas as the frontal cortex, the occipitotemporal region, the midtemporal and superior temporal cortices, the parietal/occipital cortex near the angular gyrus specialize mainly in the left hemisphere during the acquisition of reading skills (Schlaggar and McCandliss, 2007).

Concurrent occurrence of hubs in the anterior temporal lobe and visual word form areas, that was present in the controls, was not observed in children with DD (α, β1), which may be due to their ongoing development. The absence of hubs adjacent to the Heschl gyrus in children with DD has been found to be an early sign of dyslexia (Liu et al., 2015). However, the appearance of hubs in the primary sensory cortices after training suggests that the impairment in dyslexic children may be compensated by training procedures. The presence of hubs in children with developmental dyslexia after training in the dorsal visual network, including the inferior parietal, the middle temporal visual association cortex and the dorsal superior frontal cortex suggests that the training could help forward the child's development.

In general, these observations highlight the heterogeneity in the hub processing within functionally specialized brain systems and reveal how the crucial roles of distinct hubs may be disturbed by alterations to the segregation of brain systems. Effective task performance requires greater interactivity between processing hubs that are distributed across multiple brain systems accomplishing through temporary desegregation of the task-related components from the network organization including a process that can lead to greater segregation between otherwise strongly connected components. In the brain of typical children, the diverse connectivity of interconnecting hubs, engaged in a wide variety of tasks, probably mediates a broad repertoire of functions and allows them to flexibly integrate and transfer information between separate functional systems. The task-related connected and unconnected hub distinctions in connectivity patterns of the dyslexics are diminished in brain networks that exhibit less systematic segregation.

Some methodological limitations of the MST study are related to the fact that some measures are sensitive to the network size, which could affect the relative importance of the nodes in the operation of the network. The main limitation of the segregation analysis is related to the threshold selection for the hub's distribution, which highlighted the regions with a mean degree/BC at least one standard deviation above the mean value and avoided the selection of those nodes with links that had weaker intensity.

Conclusions

This study revealed an altered topological organization of the brain functional network in children with developmental dyslexia. Along with changes in regional network properties and hub distribution, the findings reveal that functional network analysis can be a promising tool for throwing light on the neuropathological mechanism of developmental dyslexia as well as post-training intervention changes. Research of functional connectivity may reveal markers of DD with promising prospects for observing remediation-related neuronal changes.

Acknowledgments: *The authors would like to express their gratitude to the psychologist Dr. Y. Lalova (Institute for Population and Human Studies) and the logopedist A. Kalonkina (State Speech Therapy Center, Ministry of Education and Science) for administering and scoring the psychological tests.*

Author contributions: *JAD was responsible for conceiving and designing this study and the training sessions. JAD was in charge of the surveys and the data acquisition. SAT designed the computer' paradigm and analyzed the data. SAT and JAD conceived the statistical analysis, wrote and revised the manuscript. JAD was responsible for the study concept, manuscript preparation, manuscript authorization, obtaining funding support. Both authors approved the final version of the manuscript.*

Conflicts of interest: *None declared.*

Financial support: *The study was supported by a grant from the National Science Fund of the Ministry of Education and Science (project DN05/14-2016, to JAD).*

Institutional review board statement: *Approval for the study was obtained from the Ethics Committee of the Institute of Neurobiology and the Institute for Population and Human Studies, Bulgarian Academy of Sciences (approval No. 02-41/12.07.2019) on March 28, 2017, and the State Logopedic Center and the Ministry of Education and Science (approval No. 09-69/14.03.2017) on July 12, 2019.*

Declaration of participant consent: *The authors certify that they have obtained all appropriate participant consent forms. In the forms the participants' parents have given their consent for the children's images and other clinical information to be reported in the journal. The participants' parents understand that the children's names and initials will not be published and due efforts will be made to conceal their identity.*

Reporting statement: *This study followed the STrengthening the Reporting of OBservational studies in Epidemiology (STROBE) statement.*

Biostatistics statement: *The statistical methods of this study were reviewed by the professor in biostatistics and neuroscience and an author of this article, Dr. Juliana Dushanova in Bulgarian Academy of Sciences, Bulgaria.*

Data sharing statement: *For data sharing, individual participant data, study protocol or informed consent will not be available. However, the details of statistical analysis plan or other information in the current study are available from the corresponding author on reasonable request.*
Plagiarism check: *Checked twice by iThenticate.*
Peer review: *Externally peer reviewed.*

Additional files:

Additional file 1: *Model consent form and subject information sheet with a design protocol.*

Additional file 2: *Ethical Approval Documentation.*

Additional file 3: *STROBE checklist.*

Additional Table 1: *Psychological tests for control and dyslexic groups in standard scores.*

Additional Table 2: *Nonparametric statistical comparison of the hubs (degree: hD; betweenness centrality: hBC) of the brain networks of control, pre-training and post-training dyslexic groups during discrimination of words.*

Additional Table 3: *Nonparametric statistical comparison of the hubs of the brain networks of control, pre-training and post-training dyslexic groups during pseudo-word discrimination.*

References

Annett M (1970) A classification of hand preference by association analysis. Br J Psychol 61:303-321.
Barrat A, Barthélemy M, Vespignani A (2008) Dynamical processes on complex networks. Cambridge: Cambridge University Press.
Bassett DS, Bullmore E (2006) Small-world brain networks. Neuroscientist 12:512-523.
Benassi M, Simonelli L, Giovagnoli S, Bolzani R (2010) Coherence motion perception in developmental dyslexia: A meta-analysis of behavioral studies. Dyslexia 16:341-357.
Binder JR, Desai RH, Graves WW, Conant LL (2009) Where is the semantic system? A critical review and meta-analysis of 120 functional neuroimaging studies. Cereb Cortex 19:2767-2796.
Boccaletti S, Latora V, Moreno Y, Chavez M, Hwanga DU (2006) Complex networks: Structure and dynamics. Phys Rep 424:175-308
Boersma M, Smit DJ, Boomsma DI, De Geus EJ, Delemarre-van de Waal HA, Stam CJ (2013) Growing trees in child brains: graph theoretical analysis of electroencephalography-derived minimum spanning tree in 5- and 7-year-old children reflects brain maturation. Brain Connect 3:50-60.
Boets B, Vandermosten M, Cornelissen P, Wouters J, Ghesquière P (2011) Coherent motion sensitivity and reading development in the transition from prereading to reading stage. Child Dev 82:854-869.
Bullmore E, Sporns O (2009) Complex brain networks: graph theoretical analysis of structural and functional systems. Nat Rev Neurosci 10:186-198.
Chouake T, Levy T, Javitt DC, Lavidor M (2012) Magnocellular training improves visual word recognition. Front Hum Neurosci 6:14.
Ebrahimi L, Pouretemad H, Khatibi A, Stein J (2019) Magnocellular based visual motion training improves reading in persian. Sci Rep 9:1142.
Farahibozorg S, Henson RN, Woollams AM, Hauk O (2019) Distinct roles for the Anterior Temporal Lobe and Angular Gyrus in the spatio-temporal cortical semantic network. bioRxiv doi: https://doi.org/10.1101/544114.
Fornito A, Zalesky A, Bullmore ET (2010) Network scaling effects in graph analytic studies of human resting-state fMRI data. Front Syst Neurosci 4:22.
Fraga González G, Van der Molen MJW, Žarić G, Bonte M, Tijms J, Blomert L, Stam CJ, Van der Molen MW (2016) Graph analysis of EEG resting state functional networks in dyslexic readers. Clin Neurophysiol 127:3165-3175.
Giacometti P, Perdue KL, Diamond SG (2014) Algorithm to find high density EEG scalp coordinates and analysis of their cor-respondence to structural and functional regions of the brain. J Neurosci Methods 229:84-96.
Girolami-Boulinier A (1985) Assessing Reading and Writing Skills (CALE). Delachaux & Niestle, Neuchatel- Paris, Masson.
Goswami U (2015) Sensory theories of developmental dyslexia: three challenges for research. Nat Rev Neurosci 16:43-54.
Habib M (2000) The neurological basis of developmental dyslexia: An overview and working hypothesis. Brain 123:2373-2399.
Hagmann P, Sporns O, Madan N, Cammoun L, Pienaar R, Wedeen VJ, Meuli R, Thiran JP, Grant PE (2010) White matter maturation reshapes structural connectivity in the late developing human brain. Proc Natl Acad Sci U S A 107:19067-19072.
Harmony T (2013) The functional significance of delta oscillations in cognitive processing. Front Integr Neurosci 7:83.
He W, Sowman PF, Brock J, Etchell AC, Stam CJ, Hillebrand A (2019) Increased segregation of functional networks in developing brains. Neuroimage 200:607-620.
Horowitz-Kraus T, Holland SK (2015) Greater functional connectivity between reading and error-detection regions following training with the reading acceleration program in children with reading difficulties. Ann Dyslexia 65:1-23.
Kalonkina A, Lalova Y (2016) Normative indicators for the test battery for a written speech assessment. Sofia, Bulgaria: Rommel Publishing House.
Koessler L, Maillard L, Benhadid A, Vignal JP, Felblinger J, Vespignani H, Braun M (2009) Automated cortical projection of EEG sensors: anatomical correlation via the international 10-10 system. Neuroimage 46:64-72.
Kruskal JB (1956) On the shortest spanning subtree of a graph and the traveling salesman problem. Proc Am Math Soc 7:48.
Lalova Y, Dushanova J, Kalonkina A, Tsokov S, Hristov I, Totev T, Stefanova M (2018) Vision and visual attention of children with developmental dyslexia. Psychol Res 21:247-261.
Lalova Y, Dushanova J, Kalonkina A, Tsokov S (2019) Application of specialised psychometric tests and training practices in children with developmental dyslexia. Psychol Res 22:271-283.
Lawton T (2011) Improving magnocellular function in the dorsal stream remediates reading deficits. Optom Vis Dev 42:142-154.
Lawton T (2016) Improving dorsal stream function in dyslexics by training figure/ground motion discrimination improves attention, reading fluency, and working memory. Front Hum Neurosci 10:397.
Lawton T, Shelley-Tremblay J (2017) Training on movement figure-ground discrimination remediates low-level visual timing deficits in the dorsal stream, improving high-level cognitive functioning, including attention, reading fluency, and working memory. Front Hum Neurosci 11:236.
Liao LD, Wang IJ, Chen SF, Chang JY, Lin CT (2011) Design, fabrication and experimental validation of a novel dry-contact sensor for measuring electroencephalography signals without skin preparation. Sensors 11:5819-5834.
Liu K, Shi L, Chen F, Waye MM, Lim CK, Cheng PW, Luk SS, Mok VC, Chu WC, Wang D (2015) Altered topological organization of brain structural network in Chinese children with developmental dyslexia. Neurosci Lett 589:169-175.
Matanova V, Todorova E (2013) DDE-2 Test Battery for Evaluation of Dyslexia of Development- Bulgarian Adaptation. Sofia, Bulgaria: OS Bulgaria Ltd.
Qian Y, Bi HY (2015) The effect of magnocellular-based visual-motor intervention on Chinese children with developmental dyslexia. Front Psychol 6:1529.
Raichev P, Geleva T, Valcheva M, Rasheva M, Raicheva M (2005) Protocol on neurological and neuropsychological studies of children with specific learning disabilities. In: Integrated Learning and Resource Teacher (Evgenieva E, ed), pp82-105. Sofia, Bulgaria: Publishing House "Dr. Ivan Bogorov".
Raven J, Raven JC, Court JH (1998) Manual for Raven's progressive matrices and vocabulary scales. Section 2: The coloured progressive matrices. Oxford, UK: Oxford Psychologists Press.
Rubinov M, Sporns O (2010) Complex network measures of brain connectivity: uses and interpretations. Neuroimage 52:1059-1069.
Sartori G, Job R, Tressoldi PE (2007) DDE-2: Battery for the assessment of developmental dyslexia and dysorthographia – 2. Florence: Giunti O.S.
Schlaggar BL, McCandliss BD (2007) Development of neural systems for reading. Annu Rev Neurosci 30:475-503.
Schurz M, Wimmer H, Richlan F, Ludersdorfer P, Klackl J, Kronbichler M (2015) Resting-state and task-based functional brain connectivity in developmental dyslexia. Cereb Cortex 25:3502-3514.
Shaywitz SE, Shaywitz BA, Pugh KR, Fulbright RK, Constable RT, Mencl WE, Shankweiler DP, Liberman AM, Skudlarski P, Fletcher JM, Katz L, Marchione KE, Lacadie C, Gatenby C, Gore JC (1998) Functional disruption in the organization of the brain for reading in dyslexia. Proc Natl Acad Sci U S A 95:2636-2641.
Smith K, Ablo D, Escudero J (2017) Accounting for the complex hierarchical topology of EEG phase-based functional connectivity in network binarisation. PLoS One 12:e0186164.
Spironelli C, Penolazzi B, Angrilli A (2008) Dysfunctional hemispheric asymmetry of theta and beta EEG activity during linguistic tasks in developmental dyslexia. Biol Psychol 77:123-131.
Sporns O (2013) Structure and function of complex brain networks. Dialogues Clin Neurosci 15:247-262.
Stam CJ, Tewarie P, Van Dellen E, van Straaten EC, Hillebrand A, Van Mieghem P (2014) The trees and the forest: Characterization of complex brain networks with minimum spanning trees. Int J Psychophysiol 92:129-138.
Stam CJ, Nolte G, Daffertshofer A (2007) Phase lag index: assessment of functional connectivity from multi-channel EEG and MEG with diminished bias from common sources. Hum Brain Mapp 28:1178-1193.
Stein J (2014) Dyslexia: the role of vision and visual attention. Curr Dev Disord Rep 1:267-280.
Tewarie P, van Dellen E, Hillebrand A, Stam CJ (2015) The minimum spanning tree: an unbiased method for brain network analysis. Neuroimage 104:177-188.
Tomasello R, Garagnani M, Wennekers T, Pulvermuller F (2017) Brain connections of words, perceptions and actions: A neurobiological model of spatio-temporal semantic activation in the human cortex. Neuropsychologia 98:111-129.
van Wijk BC, Stam CJ, Daffertshofer A (2010) Comparing brain networks of different size and connectivity density using graph theory. PLoS One 5:e13701.
Vincent JL, Kahn I, Zinder AZ, Raichle ME, Buckner RL (2008) Evidence for a frontoparietal control system revealed by intrinsic functional connectivity. J Neurophysiol 100:3328-3342.
Vogel W, Broverman DM, Klaiber EL (1968) EEG and mental abilities. Electroencephalogr Clin Neurophysiol 24:166-175.
Vourkas M, Micheloyannis S, Simos PG, Rezaie R, Fletcher JM, Cirino PT, Papanicolaou AC (2011) Dynamic task-specific brain network connectivity in children with severe reading difficulties. Neurosci Lett 488:123-128.
Watts DJ, Strogatz SH (1998) Collective dynamics of 'small-world' networks. Nature 393:440-442.
Wilmer JB, Richardson AJ, Chen Y, Stein JF (2004) Two visual motion processing deficits in developmental dyslexia associated with different reading skills deficits. J Cogn Neurosci 16:528-540.
Wolf RC, Sambataro F, Lohr C, Steinbrink C, Martin C, Vasic N (2010) Functional brain network abnormalities during verbal working memory performance in adolescents and young adults with dyslexia. Neuropsychologia 48:309-318.
World Federation of Neurology (1968) Report of research group on dyslexia and world illiteracy. Dallas: WFN.
Xia M, Wang J, He Y (2013) BrainNet Viewer: a network visualization tool for human brain connectomics. PLoS One 8:e68910.
Yakimova R (2004) Abnormalities of written speech. Sofia, Bulgaria: Rommel Publishing House.

C-Editors: Zhao M, Li CH; T-Editor: Jia Y